Journal Name

Electronic Supporting Information for

Supramolecular self-assembly of novel thermo-responsive double-hydrophilic and hydrophobic Y-shaped [MPEO-*b*-PEtOx-*b*-$(PCL)_2$] terpolymers

S. Petrova,* C. G. Venturini,* A. Jäger, E. Jäger, M. Hrubý, E. Pavlova, and P. Štěpánek

Institute of Macromolecular Chemistry, Heyrovsky Sq. 2, 162 06 Prague 6, Czech Republic.
Email: petrova@imc.cas.cz, cgventurini@gmail.com

Tel: +420 296 809 322

Characterization Techniques

The ^{1}H NMR spectra were measured with a Bruker Avance DPX 300 MHz NMR spectrometer with $CDCl_3$ as the solvent and hexamethyldisiloxane (HMDSO) as internal standard at 25 ºC. The Fourier transform infrared (FT-IR) spectra were recorded on IRAffinity-1 "Shimadzu" FT-IR spectrophotometer with MIRacle Attenuated Total Reflectance Attachment at resolution of 4 cm^{-1} accumulating 50 scans. The number-average molecular weight (M_n), weight-average molecular weight (M_w), and polydispersity index (M_w/M_n) of prepared macroinitiator, diblock copolymer and Y-shaped terpolymers were determined on a size exclusion chromatography (SEC). The analyses were performed on using the SDS 150 pump (Watrex, USA), autosampler Midas (Spark Holland) evaporatite light scattering PL ELS 1000 (Polymer Laboratories) and UV (Watrex UVD 250) detectors. The separation system consisted of two PLgel MIXED-BLS columns (Polymer Laboratories) and was calibrated with polystyrene standards (PSS, Germany). DMF was used as a mobile phase at a flow rate of 0.5 ml/min at 25 °C. Data collection and processing were done using the TriSEC (VISCOTEK Comp) software.

Dynamic (DLS) and Static (SLS) light scattering

The DLS measurements were performed using an ALV CGE laser goniometer. The scattered light of a 22 mW HeNe linear polarized laser (632.8 nm) was measured (angle 90°), and was collected on an ALV 6010 correlator. The samples were maintained at different temperatures (5-63 °C). The data were collected using the ALV Correlator Control software with a counting time of 60 s. The measured intensity correlation functions $g_2(t)$ were analysed using the algorithm REPES (incorporated in the GENDIST program) resulting in the distributions of relaxation times – $A(\tau)$. The hydrodynamic radius (R_H) of the nanoparticles was calculated from the Stokes–Einstein relation:

$$R_H = \frac{k_B T}{6\pi\eta D} \quad (1)$$

where k_B is the Boltzmann constant, T is the absolute temperature, η is the viscosity of the solvent and D is the diffusion coeficient of the nanoparticles.

The SLS measurements were carried out by varying the scattering angle from 50° to 150° with a 10° stepwise increase. The molecular weight ($M_{w(NP)}$) and the radius of gyration (R_G) of the triblock copolymer nanoparticles were estimated by:

$$\frac{Kc}{R_\theta} = \frac{1}{M_{w(NP)}}\left(1 + \frac{R_G^2 q^2}{3}\right) \quad (2)$$

where the K_c is the optical constant, R_θ is the excess normalized scattered intensity, A_2 is the second virial coefficient and the polymer concentration c is given in mg mL^{-1}. The average density of the nanoparticles (ρ) was estimated as:

$$\rho = \frac{3M_{w(NP)}}{4\pi N_A (R_H)^3} \quad (3)$$

where N_A is Avogadro's number.

Zeta Potential Measurement

Zeta potential measurement was carried out at different temperatures (5-70 °C) with Malvern Zetasizer Nano ZS instrument equipped with 4 mW He-Ne Laser (632.8 nm) based on the technique of Laser Doppler Electrophoresis.

Nanoparticle Tracking Analysis (NTA)

Analyses by NTA were carried out using the NanoSight LM10 & NTA 2.0 Analytical Software (NanoSight, Amesbury, England). The sample was diluted (1000x-Milli Q®) and injected into the sample chamber with a syringe (25 °C). This apparatus combines light scattering microscopy with a laser diode (635 nm) and a camera charge-coupled device, which allows viewing and recording the motion of nanoparticles in solution. The NTA software is able to identify and track individual nanoparticles (10-1000 nm), which are in Brownian motion, and relate their diffusion coefficient with a sphere equivalent hydrodynamic diameter as calculated using the Stokes–Einstein equation. The size distribution was expressed by the span value, calculated by Eq. (4).

$$Span = \frac{d_{(0.9)} - d_{(0.1)}}{d_{(0.5)}} \quad (4)$$

where $d_{(0.9)}$, $d_{(0.1)}$ and $d_{(0.5)}$ are the diameters at 90%, 10% and 50% cumulative volumes, respectively.

Cryo-Transmission Electron Microscopy (Cryo-TEM)

Cryo-TEM allows direct investigation of samples in the vitrified, frozen-hydrated state. 3 µL of the sample solution was applied to an electron microscopy grid covered with holey carbon supporting film (C-flat 3.5/1-4C, Electron Microscopy Science) after hydrophilization by glow discharge (Expanded Plasma Cleaner, Harrick Plasma, USA). The excess of the solution was removed by blotting (Whatman nº. 1 filter paper) for ~1 s, and the grid was immediately plunged into liquid ethane held at -181 °C. The frozen sample was immediately transferred into the microscope and observed at -173°C under the conditions described above. Cryo-TEM observations were performed on a Tecnai G2 Spirit Twin 120kV (FEI, Czech Republic), equipped with cryo-attachment (Gatan, cryo-specimen holder) using a bright field imaging mode at accelerating voltage 120 kV.

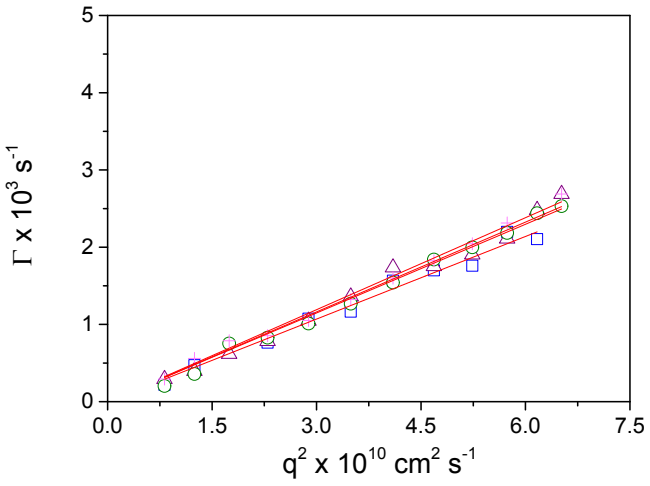

Figure S1. Relaxation rate of the [$MPEO_{44}$-*b*-$PEtOx_{252}$-*b*-$(PCL)_{2x44}$] NPs as a function of q^2 x 10^{10} cm^2 s^{-1} on the (+) 0.5 mg mL^{-1}, (○) 1.0 mg mL^{-1}, (Δ) 1.5 mg mL^{-1}, and (□) 2.0 mg mL^{-1} concentrations (25 °C).

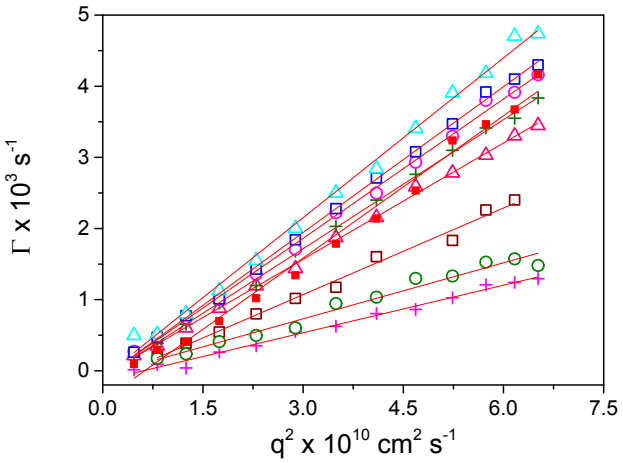

Figure S2. Relaxation rate of the [$MPEO_{44}$-*b*-$PEtOx_{252}$-*b*-$(PCL)_{2x44}$] NPs as a function of q^2 x 10^{10} cm^2 s^{-1} at the (+) 5 °C, (○) 15 °C, (□) 25 °C, (Δ) 40 °C, (+) 45 °C, (○) 50 °C, (□) 55 °C, (Δ) 60 °C, and (■) 62 °C temperatures (2 mg mL^{-1} °C).

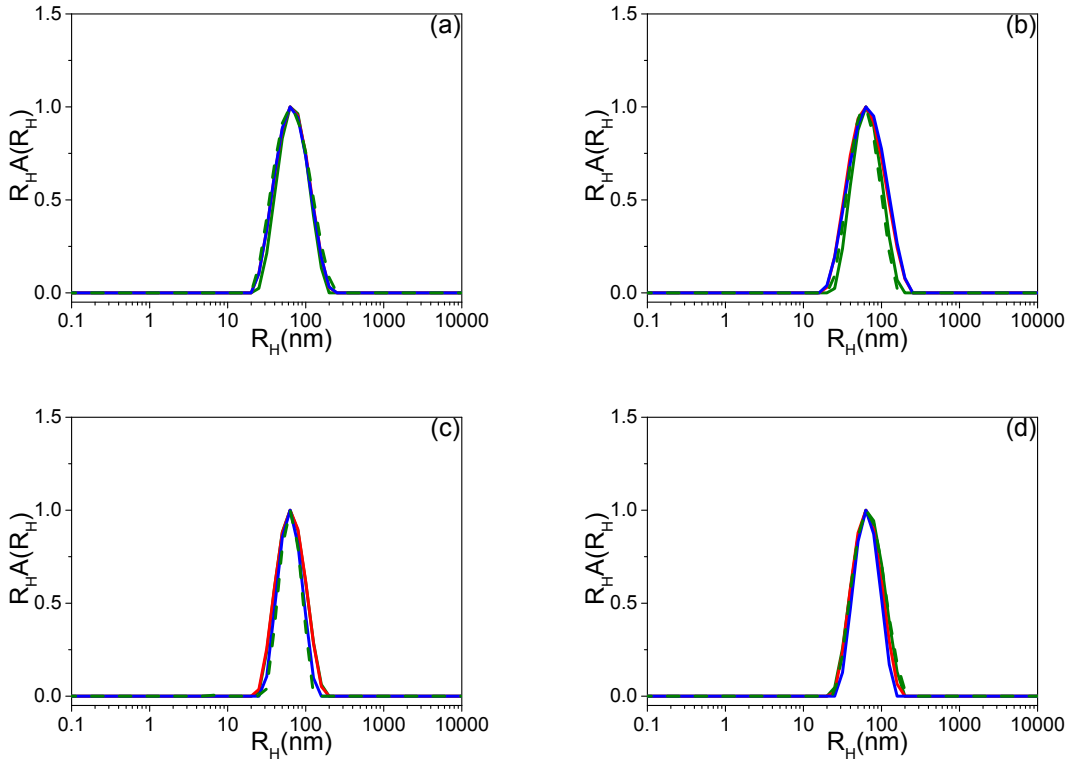

Figure S3. The distribution of the hydrodynamic radii of [$MPEO_{44}$-*b*-$PEtOx_{252}$-*b*-$(PCL)_{2x44}$] NPs solutions (PBS 7.4) on the ( ) 0.5 mg mL^{-1}, ( ) 1.0 mg mL^{-1}, ( ) 1.5 mg mL^{-1}, and ( ) 2.0 mg mL^{-1} concentrations: a) 5 °C, b) 15 °C, c) 40 °C, d) 45 °C.

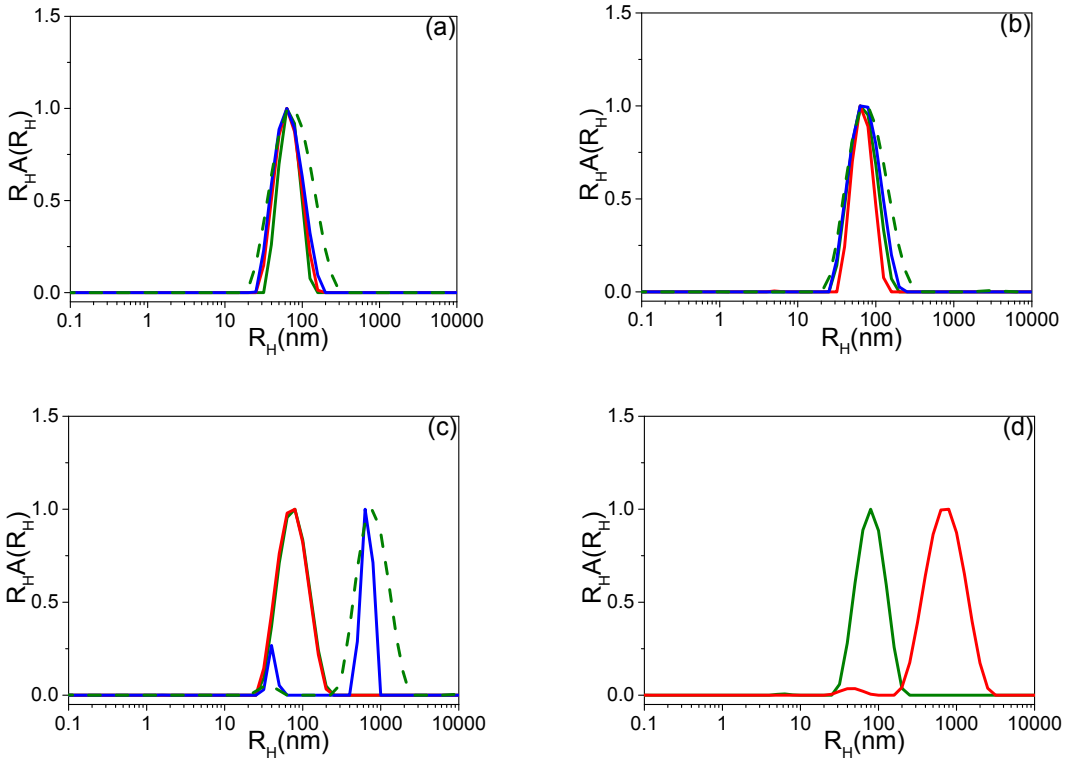

Figure S4. The distribution of the hydrodynamic radii of [$MPEO_{44}$-*b*-$PEtOx_{252}$-*b*-$(PCL)_{2x44}$] NPs solutions (PBS 7.4) on the ( ) 0.5 mg mL^{-1}, ( ) 1.0 mg mL^{-1}, ( ) 1.5 mg mL^{-1}, and ( ) 2.0 mg mL^{-1} concentrations: a) 50 °C, b) 55 °C, c) 60 °C, d) 61 °C.

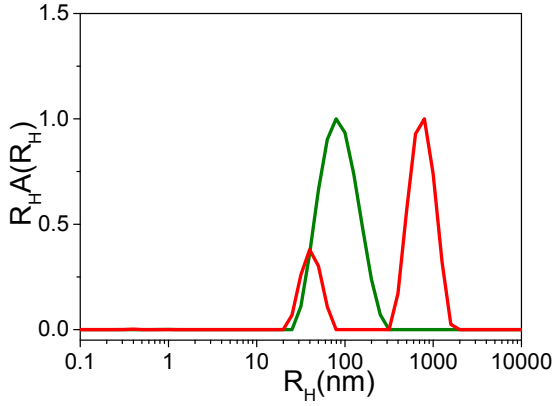

Figure S5. The distribution of the hydrodynamic radii of [$MPEO_{44}$-*b*-$PEtOx_{252}$-*b*-$(PCL)_{2x44}$] NPs solutions (PBS 7.4) on the 2.0 mg mL^{-1} concentration at ( ) 62 °C and ( ) 63 °C.

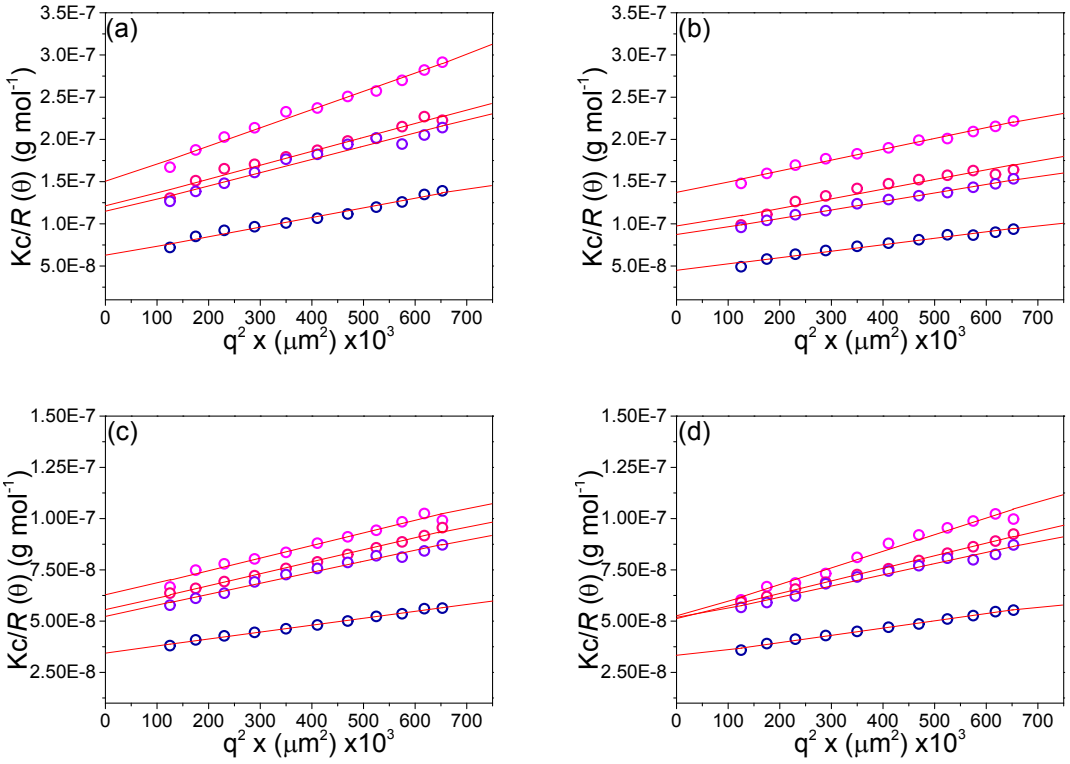

Figure S6. Rayleigh ratio dependence on q^2 on the (O) 0.5 mg mL^{-1}, (O) 1.0 mg mL^{-1}, (O) 1.5 mg mL^{-1}, and (O) 2.0 mg mL^{-1} concentrations for [MPEO$_{44}$-*b*-PEtOx$_{252}$-*b*-(PCL)$_{2x44}$] NPs: a) 5 °C, b) 15 °C, c) 40 °C, d) 45 °C.

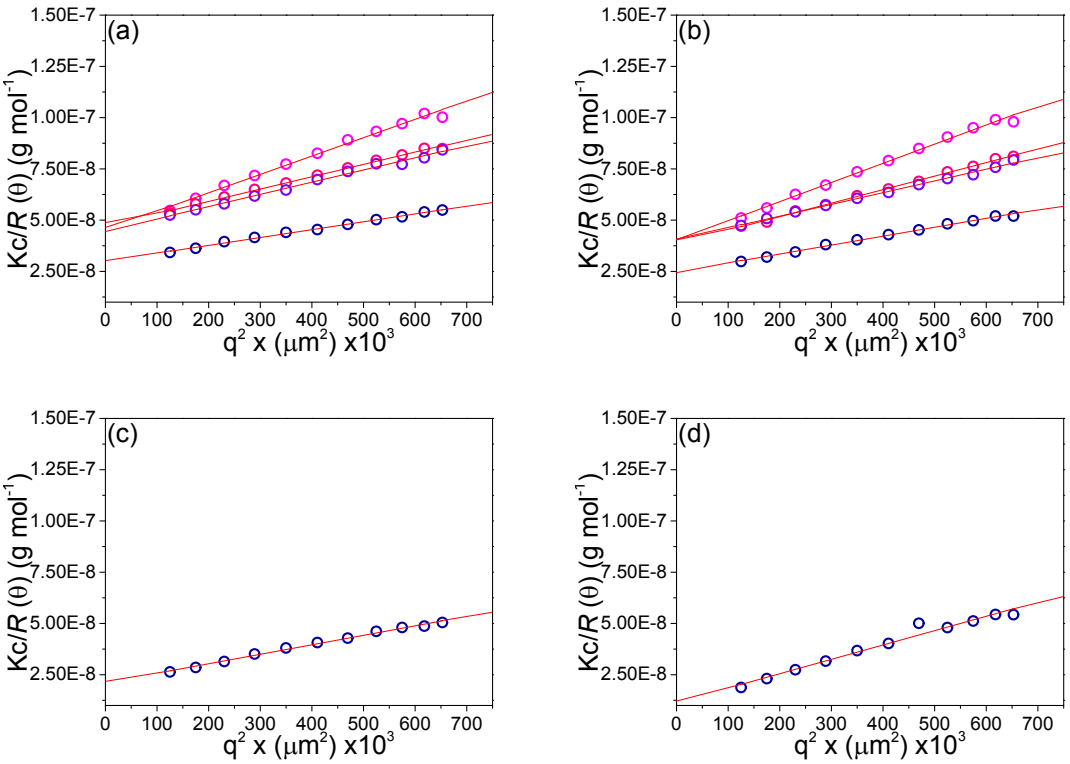

Figure S7. Rayleigh ratio dependence on q^2 on the (O) 0.5 mg mL^{-1}, (O) 1.0 mg mL^{-1}, (O) 1.5 mg mL^{-1}, and (O) 2.0 mg mL^{-1} concentrations for [MPEO$_{44}$-*b*-PEtOx$_{252}$-*b*-(PCL)$_{2x44}$] NPs: a) 50 °C, b) 55 °C, c) 60 °C, d) 62 °C.

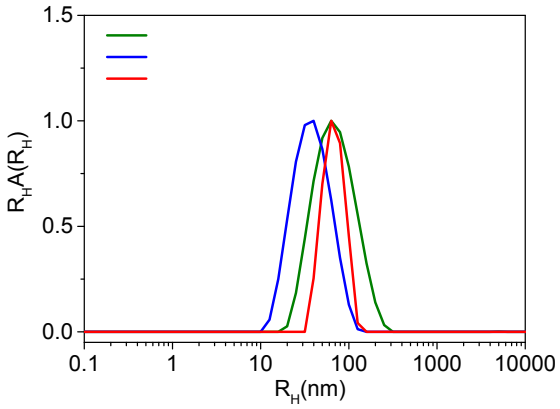

Figure S8. The distribution of the hydrodynamic radii for [$MPEO_{44}$-*b*-$PEtOx_{252}$-*b*-$(PCL)_{2x44}$] ( ) for [$MPEO_{44}$-*b*-$PEtOx_{252}$-*b*-$(PCL)_{2x87}$] (( ) and for [$MPEO_{44}$-*b*-$PEtOx_{252}$-*b*-$(PCL)_{2x131}$] ( ) NPs in PBS solutions (pH 7.4) at concentrations of 2.0 mg·mL^{-1}.

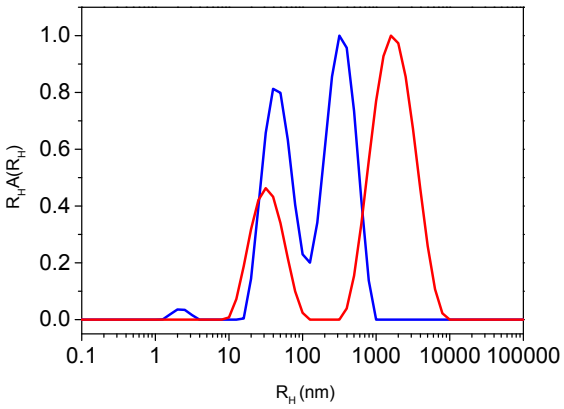

Figure S9. The distribution of the hydrodynamic radii of [$MPEO_{44}$-*b*-$PEtOx_{252}$-*b*-$(PCL)_{2x87}$] NPs solutions (PBS 7.4) on the 2.0 mg mL^{-1} concentration at ( ) 62 °C* and of [$MPEO_{44}$-*b*-$PEtOx_{252}$-*b*-$(PCL)_{2x131}$] ( ) 50 °C. *Sample precipitate immediately after measurement.